Journal of Alloys and Compounds 527 (2012) 188–192

Contents lists available at SciVerse ScienceDirect

Journal of Alloys and Compounds

journal homepage: www.elsevier.com/locate/jallcom

Effect of Zr addition and magnetic field process on the J_c property of CVD-$HoBa_2Cu_3O_{7-x}$ films

Xianping Zhang[a,c,*], Satoshi Awaji[a], Ryousuke Ishihara[a], Masafumi Namba[a], Gen Nishijima[a], Shun Ito[b], Eiji Aoyagi[b], Yanwei Ma[c], Kazuo Watanabe[a]

[a] High Field Laboratory for Superconducting Materials, Institute for Materials Research, Tohoku University, Japan
[b] Institute for Materials Research, Tohoku University, Japan
[c] Key Laboratory of Applied Superconductivity, Institute of Electrical Engineering, Chinese Academy of Sciences, China

ARTICLE INFO

Article history:
Received 24 November 2011
Received in revised form 13 February 2012
Accepted 19 February 2012
Available online xxx

Keywords:
Artificial pinning centers
Magnetic field
Nano-structures

ABSTRACT

Effects of Zr addition and magnetic field process on the superconducting property of $HoBa_2Cu_3O_{7-x}$ films fabricated by a chemical vapor deposition technique in magnetic fields have been investigated. It is found that Zr additions lead to improvement of the critical current density J_c in-field, while a further J_c enhancement along the *c*-axis of the $HoBa_2Cu_3O_{7-x}$ films is obtained in magnetic field processed samples. The nano-particles and nano-rods induced by the Zr addition are thought to account for the in-field J_c improvement. In addition, it seems that there are more columnar defects in the samples deposited under magnetic field than the normal samples, which in turn enhance the pinning ability along the *c*-axis.

1. Introduction

Remarkable progress has been made in the superconducting properties of the second generation high temperature superconductor $REBa_2Cu_3O_{7-x}$ (REBCO, RE = rare earth and Y) films in the past years [1–3]. However, the critical current density (J_c) of REBCO films still decreases rapidly as the magnetic fields increase, especially for the magnetic field parallel to the *c*-axis of the film. This restricts its practical applications such as high magnetic field coils and high quality power equipments. One of the main reasons is that the naturally induced defects along the *c*-axis are poor in as-grown REBCO thin films. Many studies in introducing artificial pinning centers (APCs), such as nano-scale impurities, columnar defects, multilayer structure and so on to the REBCO films, have been conducted [4–8]. Among them, Zr addition as an easy-to-use approach has been hotly investigated recently [9,10]. Moreover, by changing the temperature or growth rate of $BaZrO_3$-doped $YBa_2Cu_3O_7$ films in pulsed-laser deposition process, high quality films with high I_c and low anisotropy were fabricated [11].

In addition, it is well known that the magnetic field orientation effect on the basis of the magnetic anisotropy is effective for the texture control of high temperature superconductors [12,13]. If magnetic field is applied during a film deposition process, the orientation of grains and other field effects for the film growth are expected [14]. The driving force for grain alignment is provided by the anisotropy of paramagnetic susceptibility exhibited by the superconductor grains [15]. However, there is no report related to the magnetic field effect on REBCO film deposition with Zr addition.

In this paper, effects of Zr addition and magnetic field process on the microstructure and superconducting properties of $HoBa_2Cu_3O_{7-x}$ films were studied. HoBaCuO films were chosen in this work has two reasons, one is that $HoBa_2Cu_3O_{7-x}$ films have relatively high superconducting properties; the other reason is that Ho element has relatively high ferromagnetism, and as a result, the align effect of magnetic field to grains of the HoBaCuO film may be more obvious than the other ReBaCuO films. The mechanism of microstructure change by magnetic field process in the Zr added $HoBa_2Cu_3O_{7-x}$ films was analyzed.

2. Experimental details

$HoBa_2Cu_3O_{7-x}$ (HoBCO) films were grown on $SrTiO_3$ single crystal (1 0 0) substrates by the metal organic chemical vapor deposition in high magnetic fields (in-field CVD). The deposition conditions details were previously reported [16,17]. In this work, $Ho(DPM)_3$, $Ba(DPM)_2(Phen)_2$, $Cu(DPM)_2$, and $Zr(DPM)_2$ were used as source materials and set in separate furnace. The substrates were set in a vertical reactor, which was installed in the room-temperature bore of a cryogen-free superconducting magnet, and the film deposition was carried out at a constant vertical magnetic field of 0 and 8 T at 850 °C, with the surface of the substrates perpendicular to the magnetic field. Film thickness in this experiment is around 300 nm. For each same, several films were fabricated under the same condition to check reproducibility. The phase constituent and microstructure of the samples were

* Corresponding author at: Institute of Electrical Engineering, Chinese Academy of Sciences, P.O. Box 2703, BeiErTiao 6#, ZhongGuanCun, Beijing 100190, PR China. Tel.: +86 10 82547131; fax: +86 10 82547137.
E-mail address: zxp@mail.iee.ac.cn (X. Zhang).

0925-8388/$ – see front matter © 2012 Elsevier B.V. All rights reserved.
doi:10.1016/j.jallcom.2012.02.154

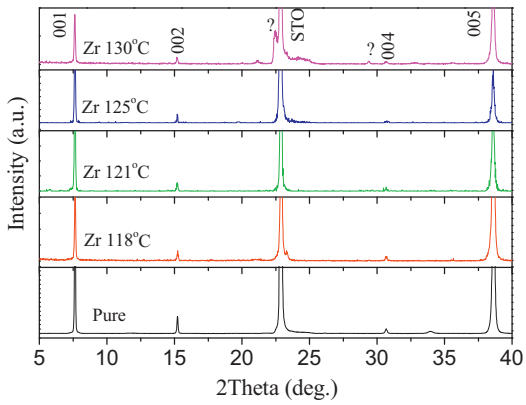

Fig. 1. XRD patterns of HoBCO films with different Zr evaporation temperature. The peaks of HoBCO phase were indexed.

investigated using X-ray diffraction (XRD), scanning electron microscopy (SEM) and transmission electron microscopy (TEM). The transport J_c at 78 K and its magnetic field dependence were evaluated by a standard four-probe technique with a criterion of 1 μV/cm in immersing liquid nitrogen. The micro-bridges, about100 μm wide and 1 mm long, were made by photolithography. Magnetic fields were applied using a 18 T cryogen-free superconducting magnet at the High Field Laboratory for Superconducting Materials (HFLSM), Institute for Materials Research (IMR), Tohoku University. The angle of the magnetic field θ was defined as the angle between the magnetic field and the *c* axis, where $B//c$ was defined as $\theta = 0^\circ$ and transport currents were always perpendicular to the magnetic field and *c*-axis.

3. Results and discussion

Fig. 1 exhibits XRD patterns ($\theta - 2\theta$ scan) of HoBCO films with different Zr evaporation temperatures (T_{zr}). It is expected that Zr addition increases with increasing T_{zr}. Regardless of the evaporation temperature of Zr, main peaks observed in the XRD pattern are corresponding to (0 0 *l*) reflections of the HoBCO phase (except the (1 0 0) peak of $SrTiO_3$ substrate) for all films, indicating that the HoBCO films have a strong *c*-axis texture [10]. However, some small impurity diffraction peaks appeared for the Zr added sample when T_{zr} reached 130 °C. This means that the amount of the impurities in this film becomes large due to the over doping of Zr. For the samples with low T_{zr}, XRD patterns were not so different from that of the pure sample, implying small impurity content in these films. These results are in accordance with the resistivity–temperature (*R*–*T*) behaviors, which will be discussed later.

Fig. 2 shows SEM images of the surfaces of HoBCO films with T_{zr} = 121 °C (a) and 125 °C (b), respectively. As can be seen from the images, typical layered grains were formed, which lie parallel to the film surface. The surface morphology of HoBCO films was very flat and almost free from hole. At the same time, some precipitates were found on the surface of these films, which are possibly CuO and Ba–Cu–O rich phases. On the other hand, it seems that Fig. 2(a) has more needle shaped *a*-axis grains, while Fig. 2(b) has more tilted grains with probably CuO underneath.

T_c of the HoBCO films fabricated with and without magnetic field was determined from the *R*–*T* curves where the resistivity is 50% of the transition. It is found that T_c of the HoBCO films were hardly affected by magnetic field applied during the film deposition process. However, for the sample with Zr evaporated at 130 °C, the critical transition temperature T_c was suppressed obviously, presumably due to the contamination of the HoBCO films by the precipitates [9], in accordance with the impurity diffraction peaks in XRD pattern. Nevertheless, for the other sample with T_{zr} lower than 130 °C, T_c is just a little lower than that of the pure sample. This means that the amount of second phases induced by Zr addition is less in these samples with lower T_{zr}.

Effect of the evaporation temperature of Zr up to 121 °C on J_c property shows a similar tendency for samples fabricated with and without magnetic field, as is evident from Fig. 3. Compared to the J_c of undoped samples, the sample with T_{zr} at 118 °C has higher J_c values in both $B//c$ and $B//ab$-plane at a low field region. Here *B* was the magnetic field applied when J_c measuring. However, the J_c was decreased with T_{zr} increasing when T_{zr} is higher than 125 °C. On the other hand, the degradation of J_c with T_{zr} increase was weakened for in-field samples, as shown in Fig. 3(b). This means that the magnetic field has a positive effect on the J_c–*B* properties of Zr doped HoBCO films [14]. As mentioned before, T_c of the HoBCO films was hardly affected by the magnetic field. So the positive effect of magnetic field may be mainly embodied on the better texture for the in-field sample than that of no-field samples.

The field dependence of J_c at 78 K for HoBCO films with T_{zr} at 118 °C is shown in Fig. 4(a). As can be seen, the J_c values of Zr doped samples are improved in both $B//c$ and $B//ab$-plane compared to those of undoped samples. For example, the $J_{c(B//ab\text{-plane})}$ value was enhanced from 3.2×10^4 A/cm^2 for undoped samples to 6.4×10^4 A/cm^2 for Zr doped samples at 5 T. Meanwhile, the J_c value was degraded at high field region. As reported in literature [18], if additional pinning centers are introduced, J_c will be enhanced in high magnetic field due to the strong flux pinning. But when the pinning strength is weak, or when the pinning density is low, artificial pinning centers cannot improve J_c in the high field region [19]. From this point, the artificial pinning centers in this experiment are still not as effective as expected. Nevertheless, the angular dependence of J_c shows obviously different behaviors for the Zr doped samples fabricated with and without magnetic field. When the magnetic field was applied during the sample fabrication process, an enhancement of J_c around the *c*-axis and a depressed J_c along the *ab*-plane was found in the Zr doped sample, which can be seen obviously from Fig. 4(b). This testifies that the enhanced

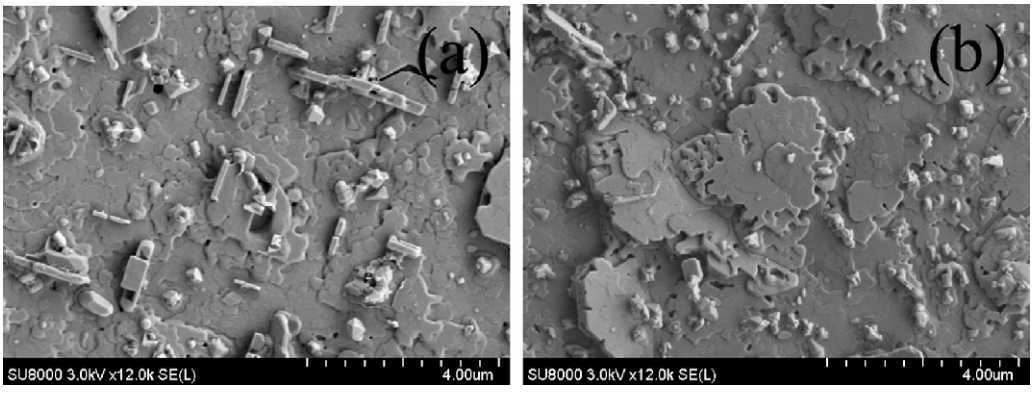

Fig. 2. SEM images of HoBCO films with Zr evaporation temperature at 121 °C (a) and 125 °C (b).

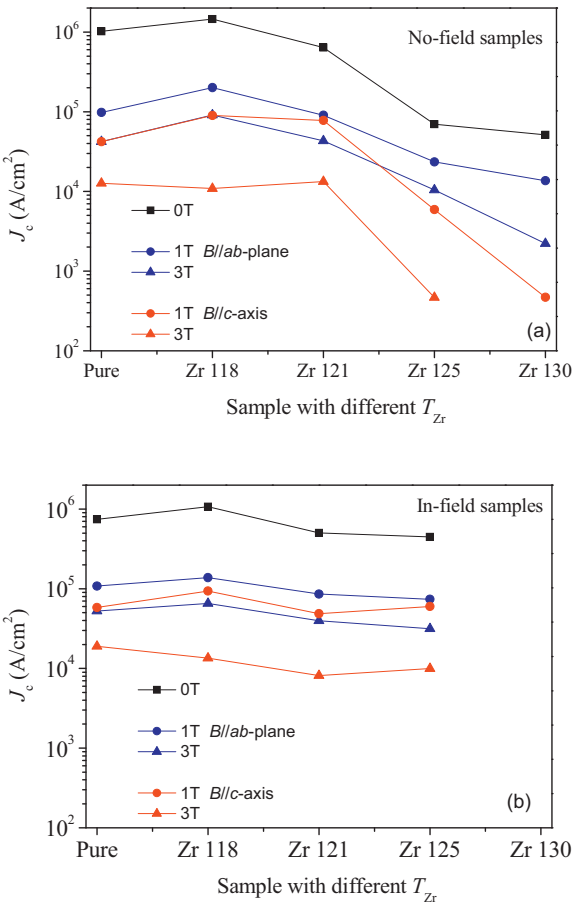

Fig. 3. J_c vs T_{zr} for HoBCO films deposited without (a) and with (b) magnetic field at 0, 1, 3 T, respectively.

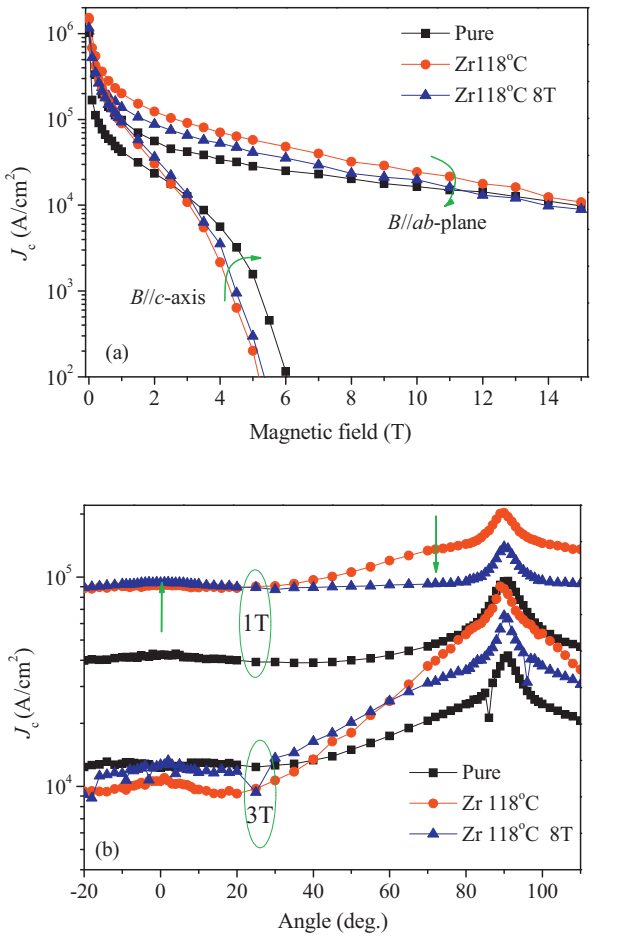

Fig. 4. The transport J_c–B properties (a) and field angular dependence of J_c at 78 K (b) of HoBCO film with T_{zr} at 118 °C.

magnetic flux pinning is due to the successful incorporation of *c*-axis correlated columnar pinning centers into the superconductor matrix, indicating that the magnetic field helps the formation of *c*-axis correlated defects, such as nano-rods, etc.

In order to identify the dimensionality of the precipitates formed in the HoBCO films, cross-sectional TEM images were taken. HoBCO films with a moderate T_{zr} = 125 °C fabricated at 0 and 8 T were selected for TEM measurement. As shown in TEM images in Fig. 5, both nano-rods and nano-particles were observed in the film matrix. Most of these inclusions are 10–20 nm in diameter, which is much larger than the typical size of the $BaZrO_3$ nano-rods and nano-particles reported previously [8,9]. These kinds of impurities and the misfit dislocations that they induce are ideal flux pinning centers, similar to the columnar defects produced by heavy-ion irradiation [20]. In particularly, the nano-rods are almost aligned along the *c*-axis of HoBCO films, which will cause aligned mismatch dislocations. This is favorable columnar pinning centers along the *c*-axis [8,21]. Nevertheless, the size and density of the nano-rods are not enough to cause the *c*-axis correlated pinning behaviors. This is the reason why the $J_{c(B//c)}$ were not obviously improved on the angular dependence of J_c as shown in Fig. 4. Fig. 6 shows the TEM planar images. Compared to the samples fabricated without magnetic field, it seems that the number of nano-rod was increased in the matrix of the in-field samples. As reported in [22], the dimensionality of the impurities in film matrix is affected by the interfacial energy between the superconducting material and the impurities. And possibly by this reason, the dimensionality of the nanoscale defects was changed due to the interfacial energy driven by the magnetic field. As a result, nano-rod density for in-field and

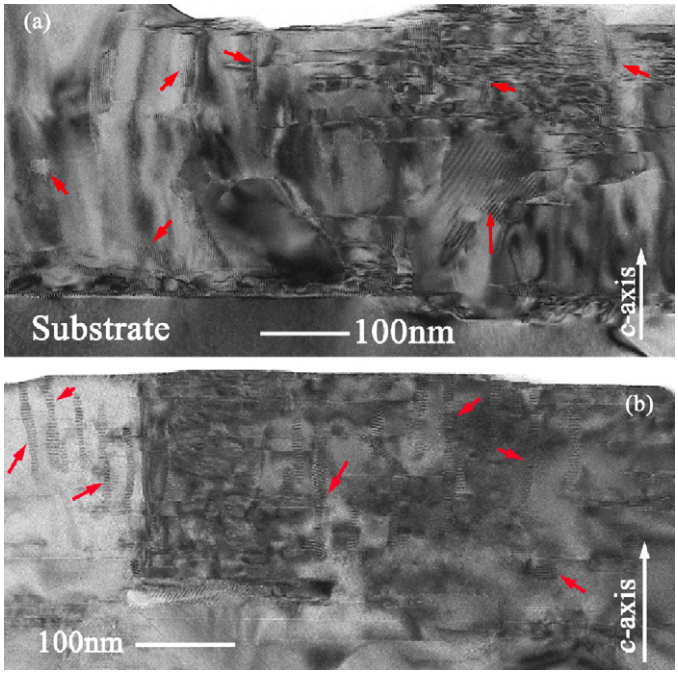

Fig. 5. TEM cross-sectional images of HoBCO film deposited without (a) and with (b) magnetic field with T_{zr} at 125 °C.

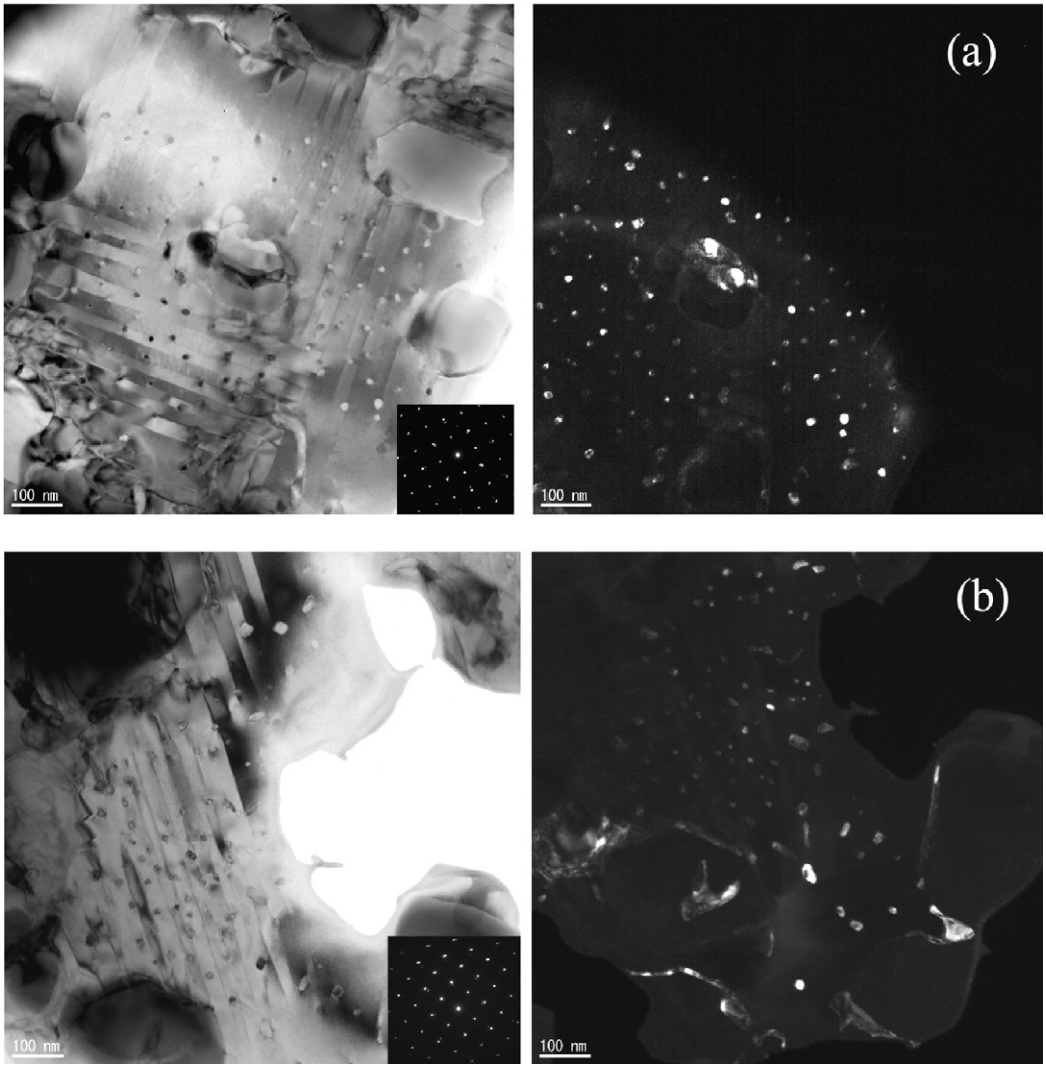

Fig. 6. TEM planar images of HoBCO film deposited without (a) and with (b) magnetic field with T_{zr} at 125 °C.

no-field samples was different. But the real mechanism about the effect of magnetic field to the defects dimensionality is still not clear.

The concept of microstructural control to improve the vortex pinning ability was introduced in early studies on metallic superconductors [22]. And the columnar defects have proven to be very effective for enhancing the pinning performance, especially for fields applied near the *c*-axis of the REBCO film [21]. From this point, the J_c enhancement by Zr addition can be explained as following: the vortex pinning ability was enhanced by the nano-inclusions produced by Zr, which can serve as pinning centers. At the same time, the increase of nano-rod density by the magnetic field is responsible for the further J_c improvement along *c*-axis for in-field samples. But as seen from HRTEM image (not shown here), some of the nano-rods have inhomogeneous diameter. Moreover, the nano-inclusions are expected to be randomly dispersed within the superconductor matrix, rather than exhibiting an optimum distribution, which will have ambiguous consequences for the analysis of the flux pinning mechanism.

What is more, it should be noted that the HoBCO films in this experiment are deposited in a special designed in-field CVD, which has more restricts than the commercial CVD or PLD machine. As a result, the J_c values of these films still have very large improvement space. More detailed discussion concerning the role of magnetic field in the nano-inclusion microstructure as well as the scaling of the nano-rods dependences on magnetic field will be the subject of future investigations.

4. Conclusions

It is found that both nano-rods and nano-particles were formed in Zr added HoBCO films. And as a result, J_c of these samples was improved, especially at a low field region. On the other hand, when the magnetic field was applied during the film fabrication process, the J_c anisotropy of the films was decreased. This possibly means that the number density of the nano-rods in the film matrix was increased by the magnetic field applied during the deposition process. Moreover, the degradation of J_c with T_{zr} increase was weakened for in-field samples, indicating a good texture of in-field samples. Further investigations on the role of magnetic field in the nano-inclusion microstructure could lead to a better understanding of the magnetic field effect on Zr doped HoBCO film, and finally obtain high J_c performance at low temperature or high temperature by introducing three-dimensional APCs or one-dimensional APCs, respectively.

References

[1] D.C. Larbalestier, A. Gurevich, D.M. Feldmann, A. Polyanskii, Nature 414 (2001) 368–377.

[2] J.L. MacManus-Driscoll, S.R. Foltyn, Q.X. Jia, H. Wang, A. Serquis, L. Civale, B. Maiorov, M.E. Hawley, M. Maley, D.E. Peterson, Nat. Mater. 3 (2004) 439–443.
[3] S.R. Foltyn, L. Civale, J.L. Driscoll-M., Q.X. Jia, B. Maiorov, H. Wang, M. Maley, Nat. Mater. 6 (2007) 631–642.
[4] P. Lu, Y.Q. Li, J. Zhao, C.S. Chern, B. Gallois, P. Norris, B. Kear, F. Cosandey, Appl. Phys. Lett. 60 (1992) 1265–1267.
[5] T. Haugan, P.N. Barnes, R. Wheeler, F. Meisenkothen, M. Sumption, Nature 430 (2004) 867–870.
[6] J. Hänisch, C. Cai, R. Hühne, L. Schultz, B. Holzapfel, Appl. Phys. Lett. 86 (2005) 122508.
[7] S.A. Harrington, J.H. Durrell, B. Maiorov, H. Wang, S.C. Wimbush, A. Kursumovic, J.H. Lee, J.L. MacManus-Driscoll, Supercond. Sci. Technol. 22 (2009) 022001.
[8] P. Mele, K. Matsumoto, T. Horide, A. Ichinose, M. Mukaida, Y. Yoshida, S. Horii, Supercond. Sci. Technol. 20 (2007) 244–250.
[9] T. Aytug, M. Paranthaman, E.D. Specht, Y. Zhang, K. Kim, Y.L. Zuev, C. Cantoni, A. Goyal, D.K. Christen, V.A. Maroni, Y. Chen, V. Selvamanickam, Supercond. Sci. Technol. 23 (2010) 014005.
[10] M. Liu, H.L. Suo, S. Ye, D.Q. Shi, Y. Zhao, L. Ma, M.L. Zhou, IEEE Trans. Appl. Supercond. 19 (2009) 3403–3406.
[11] B. Maiorov, S.A. Baily, H. Zhou, O. Ugurlu, J.A. Kennison, P.C. Dowden, T.G. Holesinger, S.R. Foltyn, L. Civale, Nat. Mater. 8 (2009) 398–404.
[12] P. Badica, K. Togano, S. Awaji, K. Watanabe, A. Iyo, H. Kumakura, J. Cryst. Growth 269 (2004) 518–534.
[13] P. Derango, M. Lees, p. Lejay, A. Sulpice, R. Tournier, M. Ingold, P. Germi, M. Pernet, Nature 349 (1991) 770–772.
[14] S. Awaji, Y.W. Ma, W.P. Chen, H. Maeda, K. Watanabe, M. Motokawa, Curr. Appl. Phys. 3 (2003) 391–395.
[15] Y.W. Ma, K. Watanabe, S. Awaji, M. Motokawa, Phys. Rev. B 65 (2002) 174528.
[16] Y.W. Ma, K. Watanabe, S. Awaji, M. Motokawa, Jpn. J. Appl. Phys. 39 (2000) L726–L729.
[17] S. Awaji, K. Watanabe, Y.W. Ma, M. Motokawa, Physica B 294 (2001) 482–485.
[18] T. Sueyoshi, K. Yonekura, R. Kajita, T. Fujiyoshi, M. Mukaida, R. Teranishi, H. Kai, K. Matsumoto, Y. Yoshida, A. Ichinose, S. Horii, S. Awaji, K. Watanabe, Physica C 469 (2009) 1396–1399.
[19] Z.J. Chen, F. Kametani, A. Gurevich, D. Larbalestier, Physica C 469 (2009) 2021–2028.
[20] N.M. Strickland, E.F. Talantsev, N.J. Long, J.A. Xia, S.D. Searle, J. Kennedy, A. Markwitz, M.W. Rupich, X. Li, S. Sathyamurthy, Physica C 469 (2009) 2060–2067.
[21] Y.X. Zhou, S. Ghalsasi, I. Rusakova, K. Salama, Supercond. Sci. Technol. 20 (2007) S147–S154.
[22] K. Matsumoto, P. Mele, Supercond. Sci. Technol. 23 (2010) 014001.